Interface birefringence in asymmetric CdTe/CdZnTe quantum wells

L. V. Kotova [1,2] A. V. Platonov [1] R. André [3] H. Mariette,[3,4] and V. P. Kochereshko [1]

[1]*Ioffe Institute, 194021 St. Petersburg, Russia*
[2]*ITMO University, 197101 St. Petersburg, Russia*
[3]*Institut Néel, CNRS, F-38000 Grenoble, France*
[4]*Japanese-French Laboratory for Semiconductor Physics and Technology J-F AST, CNRS,*
Université Grenoble Alpes, University of Tsukuba, 106-8514 Tokyo, Japan

Photoluminescence and polarized reflection spectra of quantum well structures with symmetric $Cd_{0.9}Zn_{0.1}Te/CdTe/Cd_{0.9}Zn_{0.1}Te$ and asymmetric $Cd_{0.9}Zn_{0.1}Te/CdTe/Cd_{0.4}Mg_{0.6}Te$ barriers were studied. The Stokes parameters of the reflected light from these structures were measured. In structures with asymmetric barriers, in the region of exciton resonances, the phenomenon of light birefringence was detected, caused by a lower symmetry of the interfaces compared with the symmetry of bulk crystals. A discussion of this phenomenon is given.

I. INTRODUCTION

II–VI semiconductor compounds, particularly CdTe and ZnTe, are often used for basic research. Indeed they present outstanding characteristics such as large direct band gaps (around 1.50 and 2.17 eV, respectively), large photon absorption cross sections, high atomic number, and high resistivity. These features make them also very good candidates for the following optoelectronic applications: (i) For photovoltaic conversion, the exploration of CdS/CdTe heterojunction solar cells started more than thirty years ago and the current efficiency of CdTe solar cell has reached 22.1% by the leading CdTe thin-film-based photovoltaic manufacturing company (see Refs. [1,2] and all references therein). (ii) For photodetectors applications, they cover a large range of wavelength such as x-ray or γ-ray radiation and they are nowadays already replacing other semiconductors devices [3,4].

However, one of the key issues when using heterostructures based on CdTe and ZnTe compounds is the control of mechanical stresses arising at the interfaces, which are due to the noticeable mismatch of their crystal lattices (6.4%). Moreover, due to this lattice mismatch, the magnitude of the band offset is strongly dependent on the strain. As a result, the value of the band offset is known rather approximatively ("the average valence-band offset is the algebraic sum of the chemical band offset and the hydrostatic strain contribution" [5]). For example, the scatter of published data on the band discontinuity in the valence band of CdTe/ZnTe heterostructures is up to 10% of the total band gap [5–7].

Those who manufacture heterolasers empirically know that a "good" laser will be obtained if it is fabricated, for example, in the direction [110] and a "bad" laser is fabricated in the orthogonal direction [1$\bar{1}$0]. This is partly due to the fact that these directions correspond to the directions of dislocation creation. Knowing that the interfaces are the place of maximum mismatch of the crystal lattices of the materials in contact and, consequently, the place of the dislocation origin,

the study of interface properties is therefore of crucial importance for practical tasks.

In this paper a detailed experimental study of photoluminescence and polarized reflection spectra from structures with quantum wells with symmetric and asymmetric barriers was carried out. A birefringence phenomenon caused by reduced interface symmetry in the heterostructure was found in the structure with asymmetric barriers. Previously, the manifestation of reduced interface symmetry was observed in the photoluminescence spectra of type-II heterostructures, where the exciton is "bound" directly to the interface [8–11] that is in local properties of the structures. In contrast to these publications, in this study, the reduced interface symmetry was manifested in the dielectric response of type-I structures near exciton resonances. Such a birefringence effect was also reported in type-I heterostructures by Kudelski *et al.* [12], but in their case the design of the heterostructures was such that symmetric structures were expected; only the nonabrupt interfaces and the corresponding intermixing chemical profiles were at the origin of the asymmetry. Instead, in the present paper the asymmetry is present by construction of the samples.

The paper is organized as follows: In Sec. II we describe our experiments. Section III gives a microscopic theory of excitons taking into account strain in symmetric and asymmetric quantum wells. In Sec. IV experimental results are compared with calculations which allow us to identify lines in spectra. Also, the cause of polarization conversion in the asymmetric structure is discussed and experimental results are compared with phenomenological theory. Concluding remarks are given in Sec. V.

II. EXPERIMENT

Type-I CdTe/$Cd_{0.9}Zn_{0.1}$Te-based structures with a single 8 nm wide quantum well grown by molecular-beam epitaxy in the [001] direction were investigated. Reflection high-energy electron diffraction was used to optimize the two-dimensional
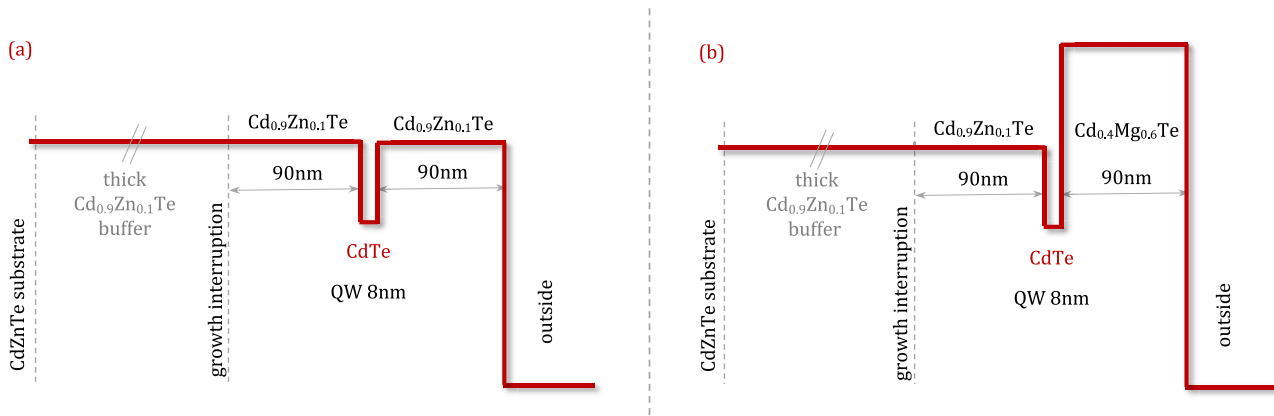
FIG. 1. The studied structures conduction band-edge energy diagram, the valence-band diagram is mirror to it. (a) Structure with a single CdTe quantum well of 8 nm width and $Cd_{0.9}Zn_{0.1}Te$ symmetric barriers of 90 nm width. (b) Structure with a single CdTe quantum well of 8 nm width and asymmetric $Cd_{0.9}Zn_{0.1}Te$ and $Cd_{0.4}Mg_{0.6}Te$ barriers of 90 nm width each. The buffer layer contains 10% of Zn and is 1.7 microns thick in both cases.

layer-by-layer growth of CdTe and the $Cd_{1-x}Zn_xTe$ alloy and to measure the layer thickness to one monolayer accuracy [13]. The structures were grown at the same time on two CdZnTe substrates having different Zn compositions (respectively 4% and 10%) on which a thick buffer layer (1.7 microns) of CdZnTe 10% Zn was deposited. Such design was chosen to have a fully relaxed buffer layer (which was checked) and to have a transparent substrate in the case of CdZnTe Zn 10% one (which allow us to perform direct absorption measurements). A set of such structures with symmetric and asymmetric barriers was fabricated. In the first case the quantum well was surrounded by symmetric barriers with 10% Zn composition on both sides, and in the second case one of the barriers was the same as in the symmetric structure, and the other barrier was based on $Cd_{0.4}Mg_{0.6}Te$ [Figs. 1(a) and 1(b)]. The height of these barriers differed by more than a factor of two. The structure parameters are given in Fig. 1.

The spectra were taken using a 0.5 m monochromator and recorded with a CCD detector. A halogen lamp was used as a light source to register transmission and reflection spectra, and a laser with wavelength of 533 nm was used for the PL spectra.

Figure 2 shows the transmission spectrum of the sample with a symmetric quantum well, with 10% Zn in the substrate, taken at 77 K. The transmission spectrum of the asymmetric sample qualitatively coincided well with this spectrum. Structures grown on substrates with a Zn composition of 4% fully absorbed light at exciton resonance energies in the quantum well. However, the reflection and transmission spectra are connected by Kramers-Kronig relations and therefore carry the same information and may well characterize these structures. In the transmission spectrum, at energy 1.595 eV a peculiarity associated with absorption to the heavy-hole exciton states in the quantum well is visible. At energies of 1.626 eV or more, absorption is observed in the $Cd_{0.9}Zn_{0.1}Te$ barrier layer. At an energy of 1.610 eV a feature related to the light hole exciton in the quantum well can be seen.

Figure 3 shows the reflection and photoluminescence (PL) spectra of the structures with symmetric and asymmetric barriers. The reflection spectra show many more features than the

absorption spectra. The main reason of it is, due to the small thickness, the exciton absorption is also small, and only states with a sufficiently large oscillator strength are visible in the absorption spectrum. The Stokes shift between the spectral features in the reflection and PL spectra is small, indicating a high quality of the structures. What is striking is that the reflection and PL spectra show too many lines for a structure with a single quantum well.

Comparing the reflection and the PL spectra of symmetric structures, we can see that some resonance features are present in the reflection spectra and absent in the PL. Usually, the opposite is the case when the lines are present in the PL spectra and absent or weak in the reflection spectra, which is associated with relaxation of carriers downward in energy. In the structure with symmetric barriers [Fig. 3(a)], there is a prominent feature in the reflection spectrum at an
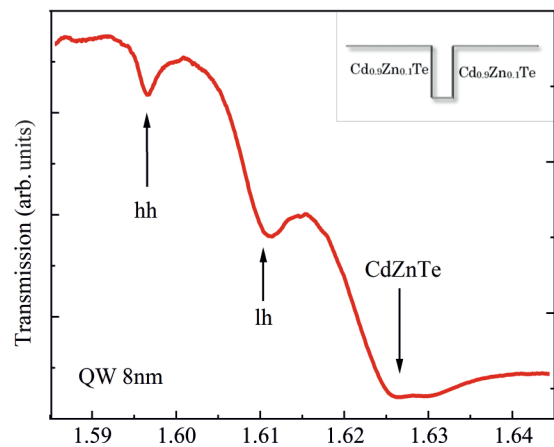
FIG. 2. Transmission spectrum of the structure with a single CdTe quantum well of 80 A width with symmetric $Cd_{0.9}Zn_{0.1}Te$ barriers, taken at 77 K. The feature at energy 1.595 eV is due to heavy-hole exciton absorption. The feature at energy 1.611 eV is related to light-hole exciton absorption. The minimum at energy 1.62 eV is associated with excitonic absorption in $Cd_{0.9}Zn_{0.1}Te$ barriers.
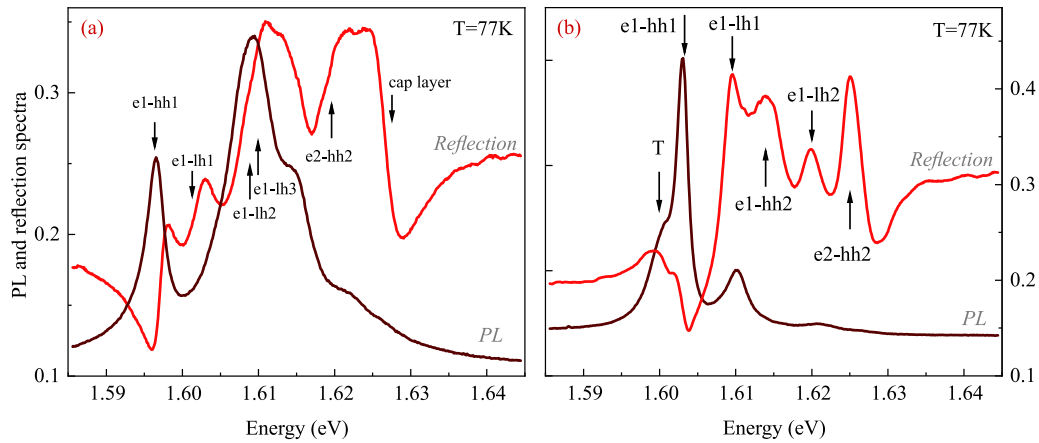
FIG. 3. Reflection and photoluminescence spectra of structures with quantum wells with (a) symmetric and (b) asymmetric barriers grown on the CdZnTe substrate with 4% Zn taken at 77 K. The arrows indicate the optical transitions to exciton states with heavy and light holes. "T" labels the trion line. The identification of these transitions was performed on the basis of calculations and described in detail in the discussion Sec. IV.

energy of 1.618 eV that is almost absent in the PL. This can only be explained by the fact that at nonresonant photoexcitation the carriers cannot populate this state, but the oscillator strength of the direct optical transition to this state is large.

The most intense line in the PL spectrum is the line at energy 1.609 eV, the intensity of the other features is remarkably lower. This indicates that relaxation into lower-energy states is difficult, and all photoexcited carriers emit through this state.

For the initial identification of the lines in the reflection spectrum, we used the result of Ref. [14] based on the shape of the exciton reflection line. In this paper, it was shown that the shape of the exciton reflection line is determined by the light interference reflected from the surface and the quantum well. Depending on the phase shift ($\varphi = kd$, k is wave vector) for the light passing the distance from the surface to the quantum well, the shape of the spectrum can change significantly. The reflection spectrum [Fig. 3(a)] shows that the contour of the exciton reflection from the surface of the structure, at energy 1.626 eV has a "differential" shape with a maximum at energy 1.624 eV and a minimum at energy 1.628 eV. The features of the reflection spectra at energies 1.597, 1.602, 1.609, and 1.620 eV have an "opposite" shape with a minimum at low energies and a maximum at higher energies. Following Ref. [14], these features should be related to the reflection from the quantum well.

A similar procedure was performed to identify the spectra of the asymmetric structure [Fig. 3(b)]. This allowed us to identify the spectral features at energies 1.604, 1.610, 1.620, and 1.625 eV as belonging to the quantum well [see the identification in Fig. 3(b)].

Polarized reflection spectra at normal and oblique light incidence from these structures were also measured. At oblique incidence of light, in both structures, the phenomenon of polarization conversion from linear to circular was observed. This phenomenon is related to the gyrotropy of quantum wells [15] and was studied in detail in our previous works [16,17]. No polarization conversion was observed in the structure with symmetric barriers at normal light incidence [17]. The degree

of circular polarization was only a few percent at oblique light incidence [17].

In Fig. 3(a), the PL line labeled e1-lh2 corresponds to two independent exciton transitions in the right and left triangular wells [Fig. 6(a)]. As shown later, the triangular shape for the well appears when the Coulombic interaction between the electron and the hole is taken into account. The parity selection rules are not followed for such wells. Therefore, the optical transitions related to these states can be quite intense in the optical spectra. The e1-hh2 transition is in resonance with e1-lh2. Perhaps the reason for their high intensity is related to the fact that lh2 and hh2 are close in energy to lh3 and hh3 with which they can mix especially in the asymmetric potential. At the same time for the e1-lh2 transition in the symmetric structure the polarization does not appear (Fig. 4) since the right and left triangular wells give an opposite in sign contribution to the polarization [18,19].
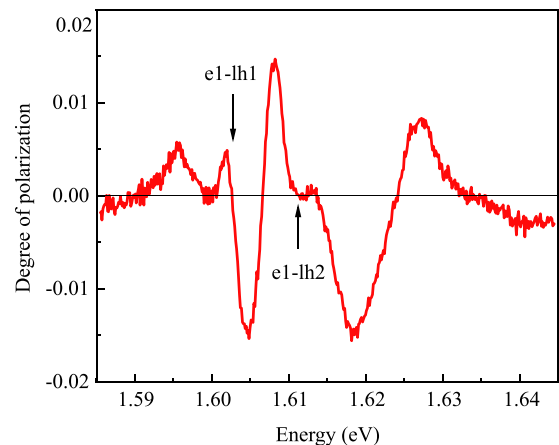
FIG. 4. Spectral dependence of the degree of circular polarization of the light reflected from a symmetric QW structure [Fig. 3(a)]. The light incident at an angle of 45° was linearly polarized in the [100] direction.
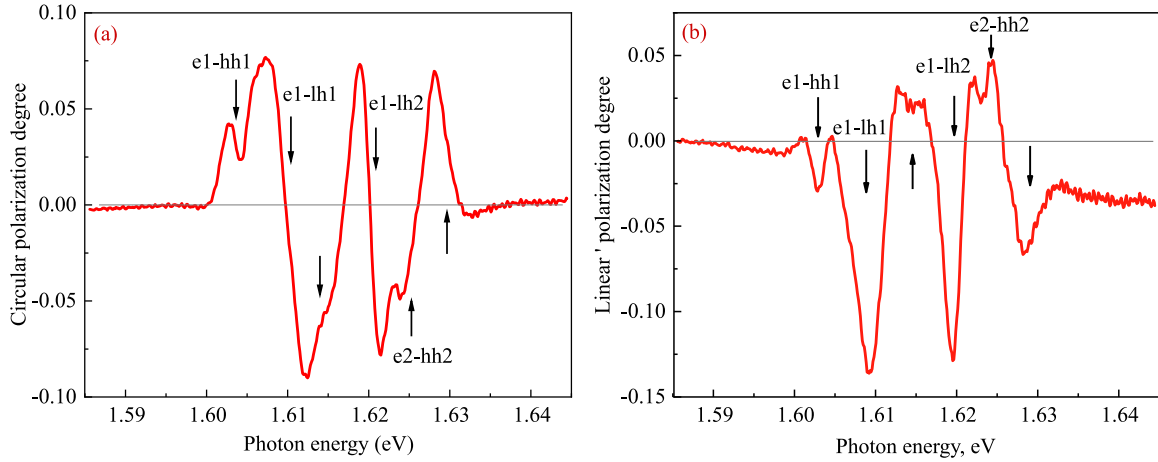
FIG. 5. Polarization degree of linearly polarized in the direction [100] light reflected from the structure with asymmetric barriers at normal incidence. (a) Degree of circular polarization, (b) degree of linear polarization in the axes rotated by 45 degrees relative to the polarization of incident light. The arrows mark the features observed in the reflection spectrum [Fig. 3(b)].

In the asymmetric structure [Fig. 3(b)], the e1-lh2 and e1-hh2 transitions are at essentially different energies. As a result, despite the effective collection to the lh2 states, the optical transition from them seen in the PL spectra is weak.

Figure 4 shows the spectral dependence of the degree of circular polarization of the reflected light, taken from a symmetric QW structure, the reflection spectrum of which, is shown in Fig. 3(a). The light incident at an angle of 45° was polarized linearly in the [100] direction. It was observed that the reflected light has a circularly polarized component with a maximum degree of polarization about 2%. This effect is due to the natural optical activity of the D_{2d} symmetric QWs; it has been described in detail in Refs. [15,17] and is not related to the anisotropy of the interfaces. Moreover, interface anisotropy can interfere with the natural optical activity.

At the same time, in the structure with asymmetric barriers, a large value of conversion, reaching nearly 10%, was found even at the normal light incidence (Fig. 5). The maximum value of circular polarization in the reflection spectrum was observed when the incident light was polarized along the [100] or [010] axis. If the incident light was polarized along the [110] or [1$\bar{1}$0] axes, the circular polarization of the reflected light did not exceed 2%.

Figure 5(a) shows the spectral dependence of the degree of circular polarization of light P_{circ} and Fig. 5(b) shows the linear polarization $P_{lin'}$ in the axes rotated by 45 degrees relative to the polarization of incident light:

$$P_{circ} = \frac{R^{\sigma^+} - R^{\sigma^-}}{R^{\sigma^+} + R^{\sigma^-}}, \quad P_{lin'} = \frac{R^{x'} - R^{y'}}{R^{x'} + R^{y'}}.$$

The spectral features of these dependencies coincide with the spectral features of the reflection spectra, as indicated by arrows in Fig. 5. Note that the minima in the dependence $P_{lin'}(\omega)$ coincide with the zeros in the dependence $P_{circ}(\omega)$.

Conversion of the linear light polarization to circular polarization in this case was directly related to the birefringence phenomenon with the optical axis along [110] or [1$\bar{1}$0]. However, despite the fact that the investigated structures were really strained, this could not lead to the appearance of an

optical axis in the plane of the structure. Indeed, birefringence emerged only in the asymmetric structure and was absent in the symmetric structure having the same mechanical stresses. It was natural to assume that the birefringence was due to the asymmetry of the interfaces. In Ref. [11] it had been shown with ZnSe/BeTe type-II quantum wells that in QWs based on cubic semiconductors with D_{2d} symmetry, each interface had C_{2v} symmetry. Such reduced symmetry could lead to interface birefringence of light. However, one wondered how an interface layer with a thickness on the order of a lattice constant could lead to such a strong effect and what role excitons played here.

In the symmetric structure [Fig. 1(a)], the potential for light holes also has a triangular shape (Fig. 6) and it would seem that interface birefringence should be observed.

To reliably identify the observed optical transitions, we performed theoretical calculations of the energies of the excitonic states.

III. THEORY

Let us estimate the positions of the lines of light- and heavy-hole excitons in this structure. The lattice constants in the materials $Cd_{0.9}Zn_{0.1}Te$ and CdTe differ by about 0.7%. As a result, in addition to the potential associated with the so-called chemical band offset between the contacting materials, the potential associated with the strain band offset acts on the carriers. The value of the chemical band offset in the valence band of $CdTe$-$Cd_{0.9}Zn_{0.1}Te$ heterostructures is known very approximately and is considered to lie in the range from -10% to $+10\%$ of the total band gap [7,11].

The value of the total chemical band offset is equal to the difference between the band gaps of the bulk materials $Cd_{0.9}Zn_{0.1}Te$ and CdTe: $\Delta = E_g^{Cd_{0.9}Zn_{0.1}Te} - E_g^{CdTe} = 0.063$ eV [20–23]. This value is divided between the conduction band (Δ_c) and the valence band (Δ_v), $\Delta = \Delta_c + \Delta_v$. In this work, we assume $\Delta_c = 0.97\Delta$ and $\Delta_v = 0.03\Delta$ [24]. Since the buffer layer and barrier layers are much thicker than the quantum well layer, we can assume that these layers are not stressed and all mechanical stresses are concentrated in the
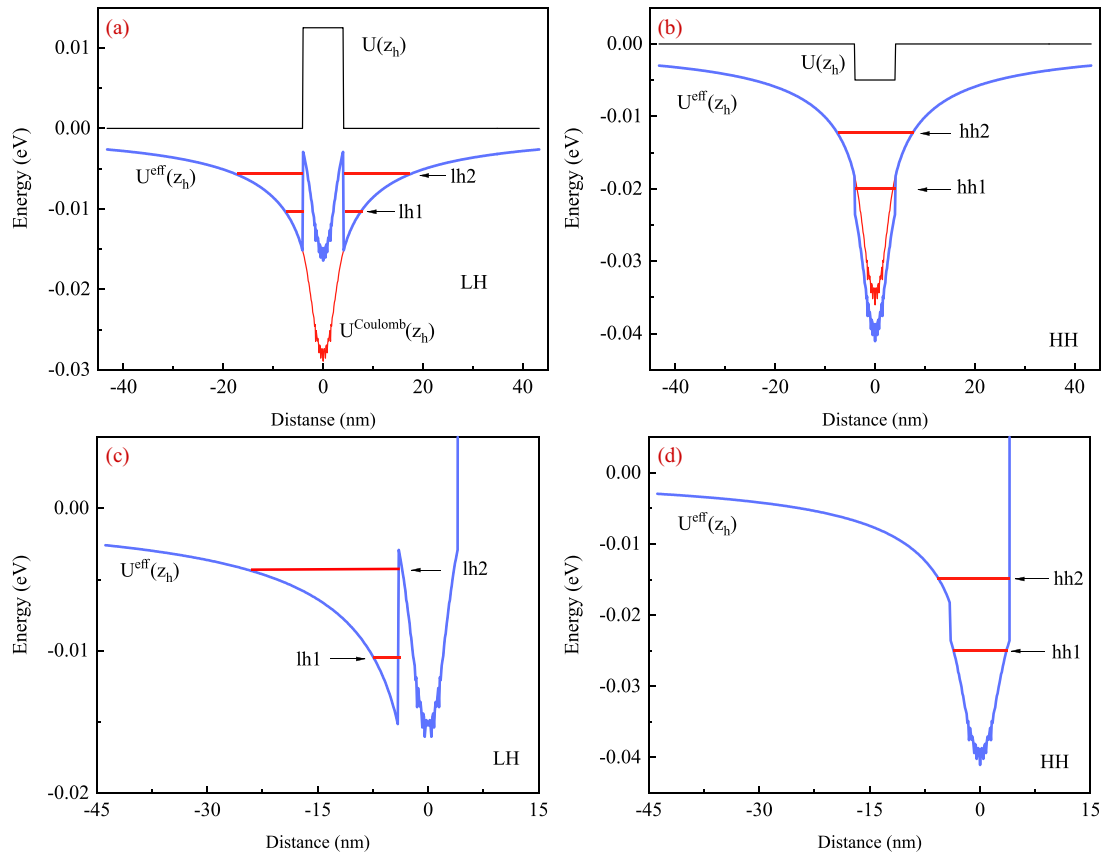
FIG. 6. Calculation of the effective potential and energy levels for hole motion created by the electron in the quantum well. $V_h(z_h)$ are nominal, rectangular potentials for heavy and light holes, without Coulomb corrections. $U^{Coulomb}(z_h)$ is averaged Coulomb potential. $V_{eff} = V_h(z_h) + R_y - U^{Coulomb}(z_h)$ is effective potential acting on the hole measured from the bottom of the valence band in CdZnTe. Panels (a) and (c) are for light holes in symmetric and asymmetric wells respectively, panels (b) and (d) are for heavy holes in symmetric and asymmetric wells, respectively.

well. The strain discontinuity of the bands can be calculated by formulas (1) [5,25]:

$$\Delta E_c = 2a_c(S_{11} + 2S_{12})\sigma,$$
$$\Delta E_{hh} = 2a_v(S_{11} + 2S_{12})\sigma + b(S_{11} - S_{12})\sigma,$$
$$\Delta E_{lh} = 2a_v(S_{11} + 2S_{12})\sigma - b(S_{11} - S_{12})\sigma. \quad (1)$$

Here ΔE_c is the deformational band offset in the conduction band, ΔE_{hh} is the deformational band offset in the heavy-hole band, ΔE_{lh} is the deformational band offset in the light-hole band, a_c and a_v are hydrostatic deformational potentials in the conduction and valence bands, b is uniaxial deformation potential, $S_{ij} \times 10^{-11}$ m^2/N are elastic constants (see Table I), $\sigma = \varepsilon/(S_{11} + S_{12})$ is mechanical in-plane tension, $\varepsilon = (a_j^L - a_i^L)/a_i^L$ is in-plane deformation.

For the deformation potentials the relations $a = a_c - a_v$, $a_c/a_v = -2$ are valid [25].

Using formula (1), we obtain that the strain band offset in the conduction band is equal to 15 meV, the strain band offset in the heavy-hole subband is equal to 2.1 meV, and the strain band offset in the light-hole subband is equal to -16.5 meV.

The deformation band offset is summed with the chemical band offset so that, for light holes, we get a type-II heterostructure due to the deformation, and for heavy holes we get a type-I structure. The band gaps at 77 K of bulk CdTe, Cd$_{0.9}$Zn$_{0.1}$Te, and Cd$_{0.4}$Mg$_{0.6}$Te are 1.585, 1.635, and 2.7 eV, correspondingly.

Since the value of the total band offset in the valence band of the studied structure is small (see Table II), the Coulomb interaction with the electron becomes the main contribution to the potential energy of holes [27].

TABLE I. Deformation potentials and elastic constants in CdTe $S_{ij} \times 10^{-11}$ m^2/N, elastic constants a, b [eV] and in-plane tension $\sigma \approx 10^{11}$ [N/m^2] [26].

S_{11}	S_{12}	S_{44}	a [eV]	b [eV]	σ
3.581	−1.394	5.5	−3.85	−1.20	0.00358

TABLE II. Total (chemical + strain) band discontinuities in CdTe/CdZnTe and CdTe/CdMgTe heterostructures [21].

CdTe/Cd$_{0.9}$Zn$_{0.1}$Te			CdTe/Cd$_{0.4}$Mg$_{0.6}$Te		
CBO	VBOhh	VBOlh	CBO	VBOhh	VBOlh
45 meV	2 meV	−12.5 meV	0.89 eV	0.22 eV	0.22 eV

We assume that the electron and hole are quantized in the potential wells for the electron and hole formed as a result of a band offset between the CdTe and CdZnTe layers and bound to each other by Coulomb interaction. The Schrödinger equation for the exciton in the simple parabolic band approximation in cylindrical coordinates has the form [28]

$$\left[-\frac{\hbar^2}{2m_e}\frac{\partial^2}{\partial z_e{}^2} + V_e(z_e) - \frac{\hbar^2}{2m_h}\frac{\partial^2}{\partial z_h{}^2} + V_h(z_h) - \frac{\hbar^2}{2\mu}\left(\frac{1}{\rho}\frac{\partial}{\partial\rho}\rho\frac{\partial}{\partial\rho} + \frac{1}{\rho^2}\frac{\partial^2}{\partial\phi^2}\right) - \frac{e^2}{\varepsilon\sqrt{\rho^2 + |z_e - z_h|^2}} \right]\Psi(\vec{r_e}, \vec{r_h})$$
$$= \left(E - \frac{\hbar^2 Q_\perp^2}{2M}\right)\Psi(\vec{r_e}, \vec{r_h}), \tag{2}$$

where

$$\phi = \arctan\left(\frac{y_e - y_h}{x_e - x_h}\right), \quad \rho = \sqrt{|x_e - x_h|^2 + |y_e - y_h|^2},$$

$V_e(z_e)$ is the rectangular potential for electrons and $V_h(z_h)$ is for holes, $V_{e,h} = 0$ inside the QW, $\mu = m_e m_h/(m_e + m_h)$ is reduced exciton mass, $M = m_e + m_h$ is total exciton mass, $Q_\perp$ is in-plane center-of-mass wave vector, ε is the static dielectric permittivity of the QW material, and E is the exciton energy in the quantum well.

For an approximate solution of equation (2), we first will solve the problem for quantization of the electron in the well and the problem for the two-dimensional exciton. Then, using the idea of the paper [27], we will find the corrections, taking into account the difference between the Coulomb potential and the purely two-dimensional potential, and then we will find the quantization levels of the hole in this potential. The radius of the two-dimensional (2D) exciton is smaller than the width of the quantum well.

As in Ref. [27], we assume that the kinetic energy of the electron in the quantum well is much greater than its binding energy of the exciton:

$$\frac{\pi^2 \hbar^2}{2m_e L^2} \gg \frac{e^2}{\varepsilon a_B},$$

L is the width of the quantum well $V_e(z_e)$, a_B is three-dimensional (3D) exciton Bohr radius ($a_B \approx 60$ Å).

Indeed, the quantization energy of an electron with effective mass $m_e \approx 0.1m_0$ in a quantum well of $L = 80$ Å width with infinite walls is $\pi^2\hbar^2/2m_e L^2 \approx 58$ meV, and the exciton binding energy is $e^2/\varepsilon a_B = Ry^{3D} \approx 10$ meV. Then the quantization energy of the electron along the z axis is the largest energy in Eq. (2). In this case, the potential acting on the hole can be averaged over the motion of the electron in z direction and in the plane.

Let us divide the Hamiltonian in Eq. (2) into two parts:

$$\left[-\frac{\hbar^2}{2m_e}\frac{\partial^2}{\partial z_e{}^2} + V_e(z_e) - \frac{\hbar^2}{2\mu}\left(\frac{1}{\rho}\frac{\partial}{\partial\rho}\rho\frac{\partial}{\partial\rho} + \frac{1}{\rho^2}\frac{\partial^2}{\partial\phi^2}\right) - \frac{e^2}{\varepsilon\rho} \right]\Psi(z_e, z_h, \rho, \phi)$$
$$+ \left[-\frac{\hbar^2}{2m_h}\frac{\partial^2}{\partial z_h{}^2} + V_h(z_h) + \frac{e^2}{\varepsilon\rho} - \frac{e^2}{\varepsilon\sqrt{\rho^2 + |z_e - z_h|^2}} \right]\Psi(z_e, z_h, \rho, \phi) = E\Psi(z_e, z_h, \rho, \phi). \tag{3}$$

All variables in the Hamiltonian in the first square bracket are separated and its eigenfunctions have the form

$$\Phi_{n,m,l}(z_e, \rho, \phi) = \varphi_n(z_e)f_{m,l}(\rho, \phi). \tag{4}$$

The functions $\varphi_n(z_e)$ describe the quantization of the electron along the z axis in the rectangular well $V_e(z_e)$.

$$\left(-\frac{\hbar^2}{2m_e}\frac{\partial^2}{\partial z_e{}^2} + V_e(z_e) \right)\varphi_n(z_e) = E_e\varphi_n(z_e). \tag{5}$$

The quantization energy of the electron in the well is found numerically, taking into account the finite height of the barriers. We neglect the tails of the electron wave function. So, the wave functions of the electron along the z axis are

$$\varphi_n(z_e) = \sqrt{\frac{2}{L}}\cos\left(\frac{\pi n}{L}z_e\right), \quad n = 1, 2, 3, \ldots.$$

The functions $f_{m,l}(\rho, \phi)$ describe the states of 2D exciton:

$$\left[-\frac{\hbar^2}{2\mu}\left(\frac{1}{\rho}\frac{\partial}{\partial\rho}\rho\frac{\partial}{\partial\rho} + \frac{1}{\rho^2}\frac{\partial^2}{\partial\phi^2}\right) - \frac{e^2}{\varepsilon\rho} - E_{m,l}^{2D} \right]$$
$$\times f_{m,l}(\rho, \phi) = 0, \tag{6}$$

where m is the main quantum number and l is the orbital quantum number $l = 0, \pm 1, \pm 2, \ldots, \pm(m-1)$. The solution for the exciton ground state is

$$f_{1,0}(\rho, \phi) = \sqrt{\frac{2}{\pi}}\frac{2}{a_B}e^{-\frac{2\rho}{a_B}} = \sqrt{\frac{2}{\pi}}\frac{1}{\tilde{a}_B}e^{-\rho/\tilde{a}_B},$$

$$E_{1,0}^{2D} = Ry^{2D} = \frac{2\mu e^4}{\hbar^2\varepsilon^2},$$

here $\tilde{a}_B = a_B/2$ is the 2D exciton Bohr radius, a_B is the bulk exciton Bohr radius [29], $a_B = \varepsilon\hbar^2/\mu e^2$.

TABLE III. Calculated exciton transition energies in the symmetric quantum well.

	e1-hh1	e2-hh2	e1-lh1	e1-lh2
Interband transitions	1.593 eV	1.620 eV	1.600 eV	1.605 eV

Let us decompose the function $\Psi(z_e, z_h, \rho, \phi)$ in Eq. (2) by the full set of functions $\Phi_{n,m,l}(z_e, \rho, \phi)$ (4):

$$\Psi(z_e, z_h, \rho, \phi) = \sum_{n,m,l} U_{n,m,l}(z_h) \Phi_{n,m,l}(z_e, \rho, \phi). \quad (7)$$

Substitute this expression into Eq. (3), multiply it by $\Phi_{n,m,l}(z_e, \rho, \phi)$ at the left side, and integrate over z_e, ρ, and ϕ. Taking into account orthogonality of $\Phi_{n,m,l}(z_e, \rho, \phi)$ we obtain the equation:

$$\left(E_n^e - E_{m,l}^{2D} - E \right) U_{n,m,l}(z_h)$$
$$= \sum_{n',m',l'} \int dz_e d\rho d\phi \, \Phi_{n,m,l}^* \left(\frac{\hbar^2}{2m_h} \frac{\partial^2}{\partial z_h^2} - V_h(z_h) - \frac{e^2}{\varepsilon \rho} \right.$$
$$\left. + \frac{e^2}{\varepsilon \sqrt{\rho^2 + |z_e - z_h|^2}} \right) U_{n',m',l'}(z_h) \Phi_{n',m',l'}. \quad (8)$$

In zero approximation, leaving only the first term in the sum, we obtain that the potential acting on the hole (*adiabatic approximation*):

$$V_{\text{eff}}(z_h) = V_h(z_h) - Ry^{2D} + \int dz_e d\rho d\phi \, \Phi_{1,1,0}^*(z_e, \rho, \phi)$$
$$\times \left(\frac{e^2}{\varepsilon \rho} - \frac{e^2}{\varepsilon \sqrt{\rho^2 + |z_e - z_h|^2}} \right) \Phi_{1,1,0}(z_e, \rho, \phi). \quad (9)$$

The summation in Eq. (8) can be continued and the result can be obtained with any accuracy (*nonadiabaticity*). For the potential acting on holes we obtain

$$V_{\text{eff}}(z_h) = V_h(z_h) + Ry^{2D} - U^{\text{Coulomb}}(z_h),$$
$$U^{\text{Coulomb}}(z_h) = \frac{e^2}{\varepsilon} \frac{2}{L} \frac{2}{\pi \tilde{a}_B^2} \int_{-L/2}^{L/2} dz_e \left| \cos \left(\frac{\pi}{L} z_e \right) \right|^2$$
$$\times \int_0^{2\pi} d\phi \int_0^\infty \rho \, d\rho e^{-2\rho/\tilde{a}_B}$$
$$\times \left[\frac{1}{\sqrt{(\rho^2 + (z_e - z_h)^2)}} \right]. \quad (10)$$

The potential $V_{\text{eff}}(z_h)$ acting on the holes is shown in Fig. 6. The hole quantization energy levels in this potential were calculated by the finite-element method.

Figure 6 shows the result of calculating the potential for holes in symmetric and asymmetric structures. The calculation is performed by calculating the potential (8) by the finite element method. The estimation of the exciton transition energies is given in Table III.

The energy of the electron at the lower quantization level in the symmetric quantum well, counted from the bottom of the CdTe well is $E_e = 20$ meV. The energy of the electron in the asymmetric quantum well is slightly higher and is equal to $E_e = 23$ meV.

Identification of the optical transitions is given in Tables IV and V.

IV. DISCUSSION

The shape of the exciton reflection line allows us to determine the distance from the surface to the quantum well [14]. Indeed, the reflection coefficient r from the structure containing the quantum well is

$$r = r_{01} + \frac{t_{01} t_{10} e^{2i\varphi}}{1 - r_{10} r_{QW} e^{2i\varphi}} * r_{QW}, \quad (11)$$

where transmittance coefficients at the vacuum-crystal interface on the crystal side is t_{10} and on the vacuum side is t_{01}; r_{01} and r_{10} are reflection coefficients at the vacuum-crystal interface on the vacuum and crystal side; r_{QW} is reflection coefficient from the quantum well, $\varphi = k(d + L/2)$ is phase shift at the passage of light from the surface to the well, k is wave vector of light, d is the distance from the surface to the quantum well.

Neglecting the multiple reflections and the quadratic on r_{QW} contribution, we obtain for the observed reflection coefficient:

$$R = |r|^2 \approx R_0 \left[1 + 2 \frac{t_{01} t_{10}}{r_{01}} \text{Re}\{r_{QW} e^{2i\varphi}\} \right], \quad (12)$$

here $R_0 = |r_{01}|^2$ is energy coefficient of reflection from the surface, t_{01}, t_{10}, and r_{01} were defined earlier. r_{01}, t_{01}, r_{10}, and t_{10} are real in the region of exciton resonance energies in the quantum well. At normal incidence $r_{01} = r_{10} = \frac{n-1}{n+1}$, $t_{01} = t_{10} = \frac{2n}{n+1}$, and n is the refractive index of light in the barriers.

Thus, the shape of the reflection spectrum is determined by the phase shift φ. The thickness of the outer barrier in our structures is 90 nm, the refractive index in CdZnTe in this spectral region is $n = 3.3$. Hence, the run-up phase of the light wave when passing the barrier layer is equal to $\phi \approx 0.8\pi$ that is close to π. That is, the shape of the exciton reflection contour from the well should be the reverse of the surface reflection contour, which can be seen in the spectra [Fig. 3(a)]. Thus, features of the reflection spectra at energies 1.597, 1.602, 1.609, and 1.620 eV should be assigned to the exciton transitions in the quantum well.

The only difference between the asymmetric and symmetric structure is that in the CdMgTe barrier layer the refractive index at the energy of exciton resonances in the quantum well is $n = 2.47$. In this case, the phase shift of the light wave as it passes through the cover layer is 0.59π that is close to $\pi/2$. This allows us to identify the spectral features at energies 1.604, 1.610, 1.620, and 1.625 eV as belonging to the quantum well. These values are slightly higher than the energies of excitonic transitions in the symmetric quantum well. Indeed, for the asymmetric well the energy level should be slightly higher than for the symmetric well. In contrast with the well with symmetric barriers in the asymmetric structure, the shape of the exciton reflection line from the CdZnTe barrier is the same as that from the quantum well. Since this

TABLE IV. Line identification. Symmetric well. Refractive index of light in the CdZnTe barrier $n = 3.3$. The reflected light phase is reversed by 180° in comparison with reflecting from the surface.

Phase [degrees]	Reflectivity [eV]	PL [eV]	Absorption [eV]	Transition
180°	1.597	1.597	1.596	e1-hh1
180°	1.6017	No	No	e1-lh1
180°	1.6091	1.610	1.610	e1-lh2 nearly coincides with e1-hh2
0°	1.615	No	No	Not identified
180°	1.620	1.620	No	e2-hh2
0°	1.626	1.626	1.626	Barrier exciton

barrier is at the same distance from the surface, the phase shift of the light wave reflected from the well and from the CdZnTe layer when passing from the well to the surface is practically the same.

Comparing the results obtained by numerical calculation, reflectance spectra, PL spectra and spectral dependencies of Stokes parameters we obtain data represented in Tables IV and V.

First of all, the question arises: why some exciton states emerge as strong features in the reflection spectra, but are completely absent in the PL spectra. Usually, it is just the opposite. Due to the energy relaxation of carriers, they accumulate in the lower-energy states, from which the PL occurs. As a result, the intensity of the PL can be significant even at low oscillator strength of the optical transition.

During nonresonant photoexcitation, holes rapidly lose energy by relaxing to the bottom of the corresponding bands. From the simple calculation follows that the QW can contain only one electron level e1. But taking into account Coulomb electron-hole interaction the transition e2-hh2 could be present like exciton excited state. In our structure, the heavy holes (hh) experience a quantum well of 2 meV depth whereas the light holes (lh) in the CdTe layers have a 12.5 meV energy barrier height (Fig. 6). From these layers, the light holes quickly move to the CdZnTe layers where their energy is lower.

Electrons arrive at the bottom of their band much later than holes. This is confirmed by their greater mobility compared with holes and, therefore, a lower rate of energy loss. Once at the lower level of dimensional quantization in the QW, they begin to bind with holes to form excitons. First, highly excited bound states with large radius are formed. Electrons and holes, emitting acoustic phonons, and then optical ones, "descend" by energy to the ground exciton state [30,31].

Those light holes that are in the CdZnTe layers at the time of electron arrival to the QW form excitons (e1-lh2). But there are no holes in CdTe layers at the moment of electrons arrival and such excitons (e1-lh1) are not formed. Thus, the holes that got into the CdTe layers before the electrons arrived cannot form excitons and such excitons are not observed in the PL spectra. However, these excitons (e1-lh1) manifest brightly in the reflection spectra since they do not require an intermediate binding and energy relaxation process for their formation (Fig. 3).

In asymmetric structures, this transition is visible in both the reflection and photoluminescence spectra. This is due to the fact that the high CdMgTe barrier effectively repels holes and does not let them escape.

Another thing that is surprising about these spectra is that the highest intensity PL peak in Fig. 3(a) identified as e1-lh2 is a nominally forbidden transition but in the second sample [Fig. 3(b)] this transition has almost zero intensity, even though the quantum well is asymmetric. In Fig. 3(a), the PL line labeled as e1-lh2 corresponds to two independent exciton transitions in the right and left triangular wells (Fig. 6). The parity selection rules are not followed for such wells. Therefore, they can be quite intense in the optical spectra. The e1-hh2 transition in the symmetric structure is in resonance with e1-lh2. As a result, on the one hand, the collection efficiency of holes into lh2 states is high, but on the other hand, the probability of their tunneling to the hh2 level is high also. That is why these optical transitions are so intense in the PL spectrum. At the same time, for the e1-lh2 transition in the symmetric structure, the polarization does not appear (Fig. 4), since the right and left triangular wells give an opposite in sign contribution to the polarization [18,19]. In the asymmetric structure [Fig. 3(b)], the e1-lh2 and e1-hh2 transitions are at essentially different energies. As a result, despite the effective

TABLE V. Line identification. Asymmetric well. Refractive index of light in the CdMgTe barrier is $n = 2.47$. The phase is modified by 90° on reflection from the QW. The CdZnTe barrier has the same phase.

Phase [degrees]	Reflectivity [eV]	PL [eV]	Transition
90°	Not identified	1.5986	Trion
90°	1.6043	1.6047	e1-hh1
90°	1.6111	1.6109	e1-lh1
90°	1.6136	1.6126	e1-hh2
90°	1.6209	1.6212	e1-lh2
90°	1.6251	No	e2-hh2
90°	1.6313	1.6303	Barrier exciton

collection to the lh2 states, the optical transition from them seen in the PL spectra is weak.

Let light, linearly polarized along axes $x\|[100]$ and $y\|[010]$, fall on the surface of the sample along axis $z\|[001]$. In this case, degree of circular polarization of reflected light is

$$2iP_{\text{circ}} = r_{x'}r_{y'}^* - r_{y'}r_{x'}^*, \tag{13}$$

where axis $x'\|[110]$ and $y'\|[1\bar{1}0]$, $r_{x'}$ and $r_{y'}$ are amplitude reflection coefficients in the axes x' and y'.

Degree of linear polarization of reflected light in the axes x' and y' rotated by 45 degrees relative to the axes x and y is

$$2P_{\text{lin}'} = r_{x'}r_{y'}^* + r_{y'}r_{x'}^*. \tag{14}$$

The degree of linear polarization in the x and y axes is

$$2P_{\text{lin}} = r_x r_x^* - r_y r_y^*. \tag{15}$$

The amplitude coefficient of exciton reflection from the quantum well is

$$r_{QW} = \frac{i\Gamma_0}{\omega_0 - \omega - i(\Gamma_0 + \Gamma)}, \tag{16}$$

where Γ_0 is radiative damping, Γ is nonradiative damping, ω_0 is the exciton resonance frequency [32].

Because of the interface anisotropy in heterostructures [11,33], the states of light and heavy holes at the interface are mixed. As a result, the reflection coefficients of light polarized along the axes [110] and [1$\bar{1}$0] in the region of exciton resonances may differ strongly. The theory predicts that the radiative damping of the exciton Γ_0 differs for these two directions, but all other exciton parameters ω_0 and Γ are the same [32]. Then, for the degree of circular polarization of the light reflected from the structure, we obtain

$$P_{\text{circ}} = \frac{\Gamma_0^{x'}\Gamma_0^{y'}\Delta\omega(\Gamma_0^{x'} - \Gamma_0^{y'})}{[\Delta\omega - i\tilde{\Gamma}^{x'}]^2[\Delta\omega - i\tilde{\Gamma}^{y'}]^2}. \tag{17}$$

Here $\Delta\omega = \omega_0 - \omega$, $\tilde{\Gamma}^{x'} = \Gamma_0^{x'} + \Gamma^{x'}$, and $\tilde{\Gamma}^{y'} = \Gamma_0^{y'} + \Gamma^{y'}$ total exciton damping.

This formula shows that the degree of circular polarization $P_{\text{circ}}(\omega)$ is zero at the resonant frequencies of the exciton. For the degree of linear polarization in the axes x' and y':

$$P_{\text{lin}'} = \frac{\Gamma_0^{x'}\Gamma_0^{y'}[(\Delta\omega)^2 + \tilde{\Gamma}^{x'}\tilde{\Gamma}^{y'}]}{[\Delta\omega - i\tilde{\Gamma}^{x'}]^2[\Delta\omega - i\tilde{\Gamma}^{y'}]^2}. \tag{18}$$

It can be seen that the degree of linear polarization in the rotated axes does not change the sign and tends to zero far from the exciton resonances.

Let us estimate these quantities. From the experimental dependence (Fig. 5) for amplitude of the linear polarization $P_{\text{lin}'}(\omega)$ we obtain

$$P_{\text{lin}'} = \left(\frac{\Gamma_0^{x'}}{\tilde{\Gamma}^{x'}}\frac{\Gamma_0^{y'}}{\tilde{\Gamma}^{y'}}\right) \approx 0.15.$$

Hence the ratio of geometric mean values is $\langle\Gamma_0\rangle/\langle\Gamma\rangle \approx 0.38$. That is, the nonradiation damping is about three times greater than the radiation damping. A similar value can be obtained from the reflection spectrum (Fig. 2). Indeed, the amplitude of the line in the reflection spectrum is $\approx \langle\Gamma_0\rangle/\langle\Gamma\rangle \approx 0.3$.

The maxima and minima in the spectral dependence $P_{\text{circ}}(\omega)$, are separated in frequency by the value $\Delta\omega \approx \Gamma$. Hence, we obtain

$$\left(P_{\text{circ}}^{\max} - P_{\text{circ}}^{\min}\right) \approx P_{\text{lin}'}^{\max}\frac{(\Gamma_0^{x'} - \Gamma_0^{y'}) + (\tilde{\Gamma}^{x'} - \tilde{\Gamma}^{y'})}{2\langle\Gamma\rangle},$$

$P_{\text{lin}'}^{\max} \approx 0.15$. We obtain $\Gamma_0^{x'}/\Gamma_0^{y'} \approx 2.5$ and $\tilde{\Gamma}^{x'}/\tilde{\Gamma}^{y'} \approx 1.5$. The value of the ratio $\Gamma_0^{x'}/\Gamma_0^{y'}$ is close to the magnitude observed in ZnSe/BeTe type-II quantum wells [34].

Such an anisotropy of the exciton radiation damping is caused by the mixing of light and heavy-hole states caused by the low symmetry of a single interface C_{2v} compared with the symmetry of the entire quantum well D_{2d}. As has been shown in Refs. [11,30,31], interface anisotropy arises due to the orientation of chemical bonds in zinc-blende based structures.

In type-II structures, the electron and hole are in different layers. In this case the exciton is localized directly at the interface itself, and the interface anisotropy manifests itself in the local properties of the structure. In our case, the anisotropy of the interfaces manifested in the anisotropy of the dielectric response; that is, in the macroscopic characteristic of the structure.

In symmetric structures, the exciton wave function "touches" both barriers. Despite the low symmetry of each of them in the quantum well, in this case, the exciton "feels" the symmetry of the whole well, i.e., the D_{2d} symmetry. In the asymmetric structure, the exciton feels stronger only one of the barriers having C_{2v} symmetry, i.e., a dedicated axis [110] in the plane of the quantum well.

V. CONCLUSION

In the present study we investigated polarized reflection spectra from structures with quantum wells having symmetrical barriers $Cd_{0.9}Zn_{0.1}Te/CdTe/Cd_{0.9}Zn_{0.1}Te$ and asymmetric $Cd_{0.9}Zn_{0.1}Te/CdTe/Cd_{0.4}Mg_{0.6}Te$. Stokes parameters of reflected light from these structures were measured. In the structures with symmetrical barriers, exciton resonances were detected in the reflection spectra, which do not show up in photoluminescence spectra. This peculiarity can be explained by the difficulty of population of some states at nonresonant optical excitation.

In the structure with asymmetric barriers in the exciton resonance region, the phenomenon of light birefringence caused by reduced symmetry of the interfaces was found. This effect was observed mainly on the light exciton states, which are due to the fact that the wave functions of light holes are in direct contact with the interfaces, while the quantization of heavy holes is determined entirely by the Coulomb field of the electron.

The birefringence phenomenon is related to the atomic structure of interfaces in heterostructures based on semiconductors with zinc-blende structure, in which the covalent chemical bonds between atoms are aligned in the directions [110] and [1$\bar{1}$0]. This results in a dedicated direction at the individual interface. The fact that an interface of infinitesimal thickness can determine the optical properties of the whole macroscopic structure is very surprising.

ACKNOWLEDGMENTS

[1] W. K. Metzger, S. Grover, D. Lu, E. Colegrove, J. Moseley, C. L. Perkins, X. Li, R. Mallick, W. Zhang, R. Malik, J. Kephart, C.-S. Jiang, D. Kuciauskas, D. S. Albin, M. M. Al-Jassim, G. Xiong, and M. Gloeckler, Exceeding 20% efficiency with in situ group V doping in polycrystalline CdTe solar cells, Nat. Energy **4**, 837 (2019).

[2] *Comprehensive Guide on Organic and Inorganic Solar Cells, Fundamental Concepts to Fabrication Methods, A volume in Solar Cell Engineering*, edited by Md. Akhtaruzzaman and Vidhya Selvanathan (Academic Press, 2022).

[3] S. N. Moger and M. G. Mahesha, Investigation on $ZnTe/Cd_xZn_{1-x}Te$ heterostructure for photodetector applications, Sens. Actuators, A **315**, 112294 (2020).

[4] M. Shkir, M. T. Khan, I. M. Ashraf, A. Almohammedi, E. Dieguez, and S. AlFaify, High-performance visible light photodetectors based on inorganic CZT and InCZT single crystals, Sci. Rep. **9**, 12436 (2019).

[5] P. Peyla, Y. Merle d'Aubigné, A. Wasiella, R. Romestain, H. Mariette, M. D. Sturge, N. Magnea, and H. Tuffigo, Exciton binding energies and the valence-band offset in mixed type-I–type-II strained-layer superlattices, Phys. Rev. B **46**, 1557 (1992).

[6] D. J. Dunstan, A. D. Prins, B. Gil, and J. P. Faurie, Phase transitions in CdTe/ZnTe strained layer superlattices, Phys. Rev. B **44**, 4017 (1991).

[7] H. Tuffigo, N. Magnea, H. Mariette, A. Wasiela, and Y. Merle d'Aubigné, Optical investigation of a strain-induced mixed type-I–type-II superlattice system: $CdTe/Cd_{1-x}Zn_xTe$, Phys. Rev. B **43**, 14629 (1991).

[8] O. Krebs and P. Voisin, Giant Optical Anisotropy of Semiconductor Heterostructures with No Common Atom and the Quantum-Confined Pockels Effect, Phys. Rev. Lett. **77**, 1829 (1996).

[9] O. Krebs, D. Rondi, J. L. Getner, L. Glodstein, and P. Voisin, Inversion Asymmetry in Heterostructures of Zinc-Blende Semiconductors: Interface and External Potential versus Bulk Effects, Phys. Rev. Lett. **80**, 5770 (1998).

[10] E. L. Ivchenko, A. A. Toropov, and P. Voisin, Interface optical anisotropy in a heterostructure with different cations and anions, Phys. Solid State **40**, 1748 (1998).

[11] A. V. Platonov, V. P. Kochereshko, E. L. Ivchenko, G. V. Mikhailov, D. R. Yakovlev, M. Keim, W. Ossau, A. Waag, and G. Landwehr, Giant Electro-optical Anisotropy in Type-II Heterostructures, Phys. Rev. Lett. **83**, 3546 (1999).

[12] A. Kudelski, A. Golnik, J. A. Gaj, F. V. Kyrychenko, G. Karczewski, T. Wojtowicz, Yu. G. Semenov, O. Krebs, and P. Voisin, Interface profiles and in-plane anisotropy in common anion type-I $Cd_{1-x}Mg_xTe/CdTe/Cd_{1-x}Mn_xTe$ heterostructures studied by reflectivity, Phys. Rev. B **64**, 045312 (2001).

[13] G. Lentz, A. Ponchet, N. Magnea, and H. Mariette, Growth control of CdTe/CdZnTe (001) strained-layer superlattices by reflection high-energy electron diffraction oscillations, Appl. Phys. Lett. **55**, 2733 (1989).

[14] E. L. Ivchenko, P. S. Kopev, V. P. Kochereshko, I. N. Uraltsev, D. R. Yakovlev, S. V. Ivanov, B. Ya. Meltser, and M. A. Kalitievskii, Reflection in the exciton region of the spectrum of a structure with a single quantum well. Oblique and normal incidence of light, Sov. Phys, Semicond. **22**, 422 (1988).

[15] L. V. Kotova, A. V. Platonov, V. N. Kats, V. P. Kochereshko, S. V. Sorokin, S. V. Ivanov, and L. E. Golub, Optical activity of quantum wells, Phys. Rev. B **94**, 165309 (2016).

[16] A.-V. V. Tsakaev and V. P. Kochereshko, Effects of spatial dispersion of excitons in quantum wells based on zinc selenide, NTV SPBTU Phys. Math. Sci. **177**, 48 (2013).

[17] L. V. Kotova, A. V. Platonov, V. N. Kats, S. V. Sorokin, S. V. Ivanov, R. Andre, V. E. Bugrov, and V. P. Kochereshko, Effects of spatial dispersion in symmetric and asymmetric semiconductor quantum wells, Phys. Status Solidi B **256**, 1800665 (2019).

[18] E. L. Ivchenko, V. P. Kochereshko, A. Yu. Naumov, I. N. Uraltsev, and P. Lavallard, Magnetic-field-effects on photoluminescence polarization in type II GaAs/AlAs superlattices, Superlattices Microstruct. **10**, 497 (1991).

[19] H. W. van Kesteren, E. C. Cosman, P. Dawson, K. J. Moore, and C. T. Foxon, Order of the X conduction-band valleys in type-II GaAs/AlAs quantum wells, Phys. Rev. B **39**, 13426 (1989).

[20] H. Mathieu, J. Allegre, A. Chatt, P. Lefebre, and J. P. Faurie, Band offsets and lattice-mismatch effects in strained-layer CdTe/ZnTe superlattices, Phys. Rev. B **38**, 7740 (1988).

[21] *Landolt-Börnstein Numerical Data and Functional Relationship in Science and Technology*, edited by W. Martienssen, Group III: Condensed Matter (Springer, 2000).

[22] E. Deleporte, J. M. Berroir, G. Bastard, C. Delalande, J. M. Hong, and L. L. Chang, Magnetic field-induced type I → type II transition in a semimagnetic $CdTeCd_{0.93}Mn_{0.07}Te$ superlattice, Superlattices Microstruct. **8**, 171 (1990).

[23] E. Deleporte, J. M. Berroir, C. Delalande, N. Magnea, H. Mariette, J. Allegre, and J. Calatayud, Excitonic effects in separate-confinement quantum-well heterostructures CdTe/(Cd, Zn)Te, Phys. Rev. B **45**, 6305 (1992).

[24] N. G. Filosofov, A. Y. Serov, G. Karczewski, V. F. Agekian, H. Mariette, and V. P. Kochereshko, Excitons in CdTe/ZnTe heterostructure with atomically thin CdTe layers, AIP Adv. **10**, 085224 (2020).

[25] H. Mariette, F. Dal'bo, N. Magnea, G. Lentz, and H. Tuffigo, Optical investigation of confinement and strain effects in $CdTe/Cd_{1-x}Zn_xTe$ single quantum wells, Phys. Rev. B **38**, 12443 (1988).

[26] D. G. Thomas, Excitons and band splitting produced by uniaxial stress in CdTe, J. Appl. Phys. **32**, 2298 (1961).

[27] Al. L. Efros, Excitons in the structures with quantum wells, Sov. Phys. Semicond. **20**, 808 (1986).

[28] G. Bastard, *Wave Mechanics Applied to Semiconductor Heterostructures, Les éditions de physique* (1992).

[29] T. Shibuya and C. E. Wulfman, The Kepler problem in two-dimensional momentum space, Am. J. Phys. **33**, 570 (1965).

[30] I. L. Aleiner and E. L. Ivchenko, Anisotropic exchange splitting in type-II GaAs/AlAs superlattices, JETP Lett. **55**, 692 (1992).

[31] E. L. Ivchenko, A. Yu. Kaminski, and I. L. Aleiner, Exchange splitting of excitonic levels in types I and II superlattices, JETP **77**, 609 (1993).

[32] E. L. Ivchenko, *Optical Spectroscopy of Semiconductor Nanostructures* (Alpha Science Int., Harrow, 2005).

[33] V. N. Abakumov, L. N. Kreshchuk, and I. N. Yassievich, Carrier capture by attractive centers in strong electric fields, Sov. Phys. Semicond. **12**, 152 (1977).

[34] A. S. Gurevich, V. P. Kochereshko, A. V. Platonov, A. Waag, D. R. Yakovlev, and G. Landwehr, Anisotropy of optical constants of ZnSe/BeTe heterostructures with no common atoms at the interfaces, Phys. Solid State **46**, 780 (2004).